

Article

Future Projection of Drought Risk over Indian Meteorological Subdivisions Using Bias-Corrected CMIP6 Scenarios

Anil Kumar Soni ¹, Jayant Nath Tripathi ¹, Mukul Tewari ^{2,*}, M. Sateesh ³ and Tarkeshwar Singh ⁴¹ Department of Earth and Planetary Sciences, University of Allahabad, Prayagraj 211002, Uttar Pradesh, India² IBM Thomas J. Watson Research Centre, Yorktown Heights, NY 10598, USA³ Climate Change Center, King Abdullah University of Science and Technology, Thuwal 23955, Saudi Arabia⁴ Nansen Environmental and Remote Sensing Centre, Bjerknes Centre for Climate Research, 5007 Bergen, Norway

* Correspondence: mtewari@us.ibm.com

Abstract: This study presents a comprehensive analysis of extreme events, especially drought and wet events, spanning over the past years, evaluating their trends over time. An investigation of future projections under various scenarios such as SSP-126, SS-245, and SSP-585 for the near (2023–2048), mid (2049–2074), and far future (2075–2100) using the bias-corrected Coupled Model Intercomparisons Project 6 (CMIP6) multi-model ensemble method was also performed. The Standard Precipitation Index (SPI), a simple yet incredibly sensitive tool for measuring changes in drought, is utilized in this study, providing a valuable assessment of drought conditions across multiple timescales. The historical analysis shows that there is a significant increase in drought frequency in subdivisions such as East MP, Chhattisgarh, East UP, East Rajasthan, Tamil Nadu, and Rayalaseema over the past decades. Our findings from a meticulous examination of historical rainfall trends spanning from 1951 to 2022 show a noticeable decline in rainfall across various regions such as Uttar Pradesh, Chhattisgarh, Marathwada, and north-eastern states, with a concurrent increase in rainfall over areas such as Gujarat, adjoining regions of West MP and East Rajasthan, and South Interior Karnataka. The future projection portrays an unpredictable pattern of extreme events, including droughts and wet events, with indications that wet frequency is set to increase under extreme SSP scenarios, particularly over time, while highlighting the susceptibility of the northwest and south peninsula regions to a higher incidence of drought events in the near future. Analyzing the causes of the increase in drought frequency is crucial to mitigate its worst impacts, and recent experiences of drought consequences can help in effective planning and decision-making, requiring appropriate mitigation strategies in the vulnerable subdivisions.

Keywords: standard precipitation index; JJAS; Indian summer monsoon (ISM); CMIP6; GCM; SSP scenarios



Citation: Soni, A.K.; Tripathi, J.N.; Tewari, M.; Sateesh, M.; Singh, T. Future Projection of Drought Risk over Indian Meteorological Subdivisions Using Bias-Corrected CMIP6 Scenarios. *Atmosphere* **2023**, *14*, 725. <https://doi.org/10.3390/atmos14040725>

Academic Editor: Ognjen Bonacci

Received: 20 March 2023

Revised: 16 April 2023

Accepted: 16 April 2023

Published: 17 April 2023



Copyright: © 2023 by the authors. Licensee MDPI, Basel, Switzerland. This article is an open access article distributed under the terms and conditions of the Creative Commons Attribution (CC BY) license (<https://creativecommons.org/licenses/by/4.0/>).

1. Introduction

India is a predominantly agricultural economy; hence, farm growth and production contributes to a large proportion (13.7%) of the country's GDP [1]. Rainfall during the Indian Summer Monsoon (ISM) from June to September is paramount for supplying water for agriculture and other living needs. ISM rainfall varies significantly in the spatiotemporal domain, resulting in severe occurrences of extreme events such as drought and flooding. As we know, drought has more sensitive and severe influences across a vast region and time frame compared to extreme flood events. Thus, drought is an intricate recurrent phenomenon [2,3] caused by a lack of precipitation or a change in the distribution of precipitation over time, which often results in the water availability. It is a slowly evolving phenomena [4,5] that impacts a large population's availability of food and water, propagates across the whole hydrological cycle, and causes long-term economic losses. In many districts (>80%) of the country, the frequency of moderate droughts, severe droughts,

and extremely severe droughts have been recorded to be greater than 9%, 6%, and 3%, respectively [6].

It is important to point out that the uncertainty of drought occurrence, its frequency, and its severity have increased in recent decades [6–11]. It is expected to increase in the future under various climate change impacts [12,13], while there is a slight change in seasonal or annual rainfall but a significant change in wet and dry days [14–16].

Since shortfall in precipitation is the primary cause of drought, there are a number of indicators that have been developed to quantify the severity of the drought which are helpful in assessing the conditions of the drought in the region. Kchouk et al. (2021) [17] discussed about 32 well-established drought indicators that are linked to three types of droughts: meteorological drought (9 indices), soil moisture/agricultural drought (15 indices), and hydrological drought (8 indices). The most often used drought indicators among them are meteorological, followed by agricultural or soil moisture, and hydrological droughts. The Standard Precipitation Index (SPI) is the most often used indicator, followed by the Normalized Difference Vegetation Index (NDVI). Based on the SPI rainfall indicator, there were 23 deficient monsoon years (all India SPI ≤ -1.0) during the period 1901–2010. Three years, 1972, 2002, and 1987, were severe drought years with drought areas of 63.4%, 42.6%, and 40.6%, respectively [6], and among them, year 1987 was one of the worst severe drought years in the past 110-year history (1901–2010). The trend study of drought intensity and the affected area in two periods, 1901–1955 and 1956–2010, indicates that during the first period, the intensity and area were decreasing with time; however in the later period, the severity and area increased [6,18].

Currently, Global Circulation Models (GCMs) are used to investigate the potential effects of climate change under various scenarios of future projections on the Indian Summer Monsoon. Coupled Model Intercomparison Project 6 (CMIP6) epitomizes the most recent advancement in GCM developments [19,20]. Some studies indicate that the CMIP6 model's seasonal mean rainfall is quite improved by 40% as compared to the previous version, CMIP5, over the Indian Summer Monsoon (ISM) and demonstrates a better spatial correlation with observations [21–24]. RCM's upgraded version (CMIP6) has better emissions, model parametrization, physical processes, land use, and land cover under different shared socioeconomic pathways (SSPs) [25,26]. Numerous studies have been carried out on drought events projections and its future impacts on population, crop yields, and others using the outputs of CMIP6 [27–35]. Most studies have mainly focused on larger regions, such as the country level or India's homogeneous region level, with less emphasis on the more granular levels, such as districts or meteorological subdivisions. However, these more detailed levels are crucial for improving drought assessments and developing effective mitigation plans.

In the present study, the historical drought pattern and the likelihood of future drought risk have been investigated at the Indian meteorological subdivision level. With the aim of contributing to the understanding of future drought patterns over the Indian region, this work utilized bias-corrected precipitation from the CMIP6 model and computed a bias-corrected ensemble GCM SPI index to determine the future changes of the drought index under the various climate scenarios during the near future (2023–2048), mid future (2049–2074), and far future (2075–2100). The paper is organized as follows: Section 2 describes the datasets and methods followed by Section 3 which consists of the results. The summary and conclusions are given in Section 4.

2. Materials and Methods

2.1. Study Area

The primary focus of this study is on the Indian subcontinent, spanning from latitude 7.5° to 37.5° N and longitude 67.5° to 97.5° E. India's climate is exceptionally diverse owing to its extensive geographical size and varied topography. The Indian climate can be broadly classified into four seasons: winter (December to February), pre-monsoon (March to May), monsoon (June to September), and post-monsoon (October to November) [6]. The

southwest monsoon season is particularly important for agriculture and water resources in India, as some regions receive up to 75% of their annual rainfall during this time and it is a key factor in determining the country's overall annual rainfall.

The Indian climate can be classified region-wise into tropical, subtropical, and arid/semi-arid regions [6]. The tropical regions are mainly located in the southern and eastern parts of the country and experience high temperatures throughout the year. These areas receive heavy rainfall during the monsoon season, making them more susceptible to flooding. Subtropical regions, located in the northern and central parts of the country, experience seasonal temperature variations with hot summers and cold winters. These regions also receive rainfall mainly during the monsoon season, but in lower amounts than the tropical regions. As a result, these regions are prone to both droughts and floods. Arid or semi-arid regions are primarily located in the northwest and western parts of the country and receive low and erratic rainfall throughout the year. These areas are highly susceptible to drought and water scarcity. India is divided into 4 homogeneous regions and further divided into 36 meteorological subdivisions based on its rainfall pattern, as shown in Figure 1.

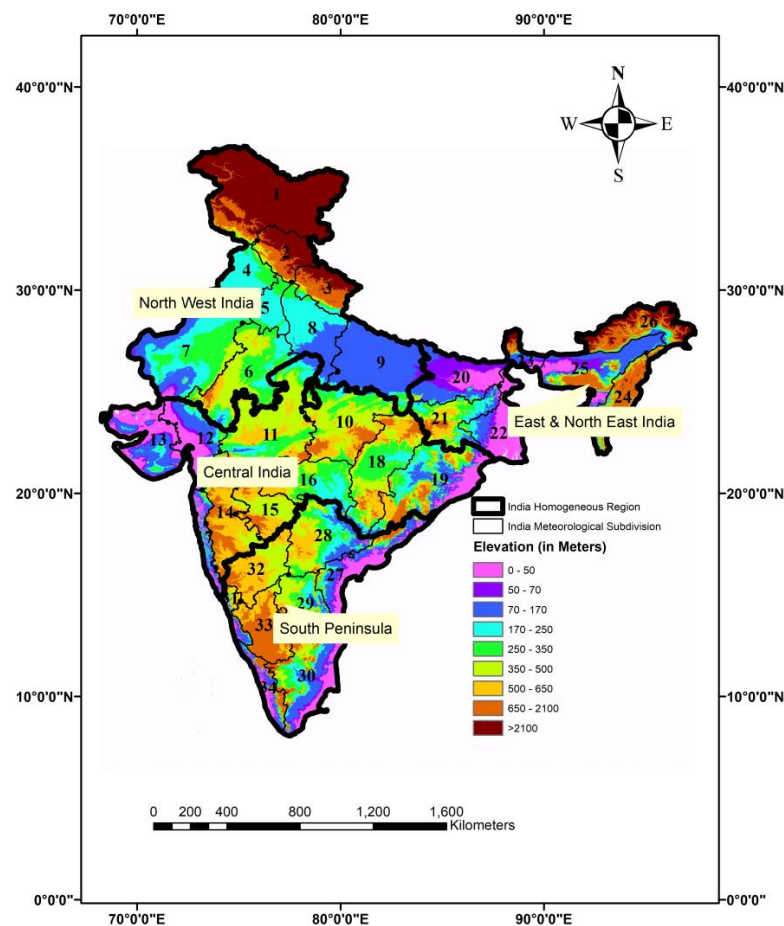


Figure 1. Map showing the study area and elevation information (in meters). **Homogenous** and Met subdivisions are **Northwest India** (Jammu and Kashmir (1), Himachal Pradesh (2), Uttarakhand (3), Punjab (4), Haryana (5), East Rajasthan (6), West Rajasthan (7), West UP (8), East UP (9)), **Central India** (East MP (10), West MP (11), Gujarat Region (12), Sourashtra (13), Madhya Maharashtra (14), Marathwada (15), Vidarbha (16), Conkan and Goa (17), Chhattisgarh (18), Odisha (19)), **East and Northeast India** (Bihar (20), Jharkhand (21), Gangetic WB (22), SHWB (23), NMMT (24), Assam and Meghalaya (25), Arunachal Pradesh (26)), **South Peninsula** (Coastal AP (27), Telangana (28), Rayalaseema (29), Tamil Nadu (30), Coastal Karnataka (31), N.I. Karnataka (32), S.I. Karnataka (33), Kerala (34)).

2.2. Observation Datasets

Observed reliable and high spatial rainfall data are crucial for the accurate assessment of drought. In this study, we used a daily gridded rainfall dataset from the National Climate Centre (NCC) of the India Meteorological Department (IMD) for the period of 1951–2022 (<https://www.imdpune.gov.in/lrfindex.php> (accessed on 15 October 2022)) over the Indian region, which is available at a daily frequency with $0.25^\circ \times 0.25^\circ$ (~625 km²) spatial resolution [36]. This gridded dataset is prepared from more than 6955 rain gauge stations. According to Pai et al. (2014) [36], the accuracy of IMD gridded data is close to the observations in heavy rainfall areas such as the west coast and over the northeast, and decreased rainfall in the leeward side of the Western Ghats (orography of the Indian subcontinent is shown in Figure 1). Researchers [36,37] have evaluated and found it more appropriate with reference to the previous resolutions of IMD gridded data and APHRODITE [38,39].

2.3. Model Datasets

Coupled Model Intercomparison (CMIP6) model data are utilized in this study for the future drought assessment and projections on various Shared Socioeconomic Pathways (SSPs). The Coupled Model Intercomparison (CMIP) project is currently in its sixth phase (CMIP6) [19,20,25] and it consists of a collection of climate model output data from various research agencies in different countries that participated in the project. These climate models simulate the Earth's climate system under different scenarios of greenhouse gas emissions and other drivers considering changes in land use, land cover, and atmosphere composition. The current CMIP6 version focuses on shared Socioeconomic Pathways (SSP1-2.6, SSP2-4.5, SSP4-6.0, and SSP5-8.5), whereas previous versions focused on future greenhouse gas emissions and included four representative concentration pathways: RCP 2.6, RCP 4.5, RCP 6.0, and RCP 8.5. For this study on the Indian climate and future drought projections, the most recent version (CMIP6) of the monthly precipitation data was downloaded from the Earth System Grid Federation ESGF (<https://esgf-node.llnl.gov/search/cmip6/> (accessed on 1 September 2022)). We obtained model data for historical and shared socioeconomic pathways (SSP1-2.6 [sustainable development pathway scenario with a goal of holding increase in global temperature below 2 °C], SSP2-2.45 [middle-of-the-road pathway scenario with medium challenge in mitigation and adaptation], and SSP5-5.85 [high emissions scenario with high challenge to mitigation and low challenge to adaptation]) [20], in which historical data are used to estimate the value of the bias correction factor, and the same is applied on the future SSPs projections to remove the model bias. A list of the CMIP6 models, their institute, countries, variant, and horizontal resolution are shown in Table 1. The mean spatial rainfall patterns of each model differ, requiring bias correction with observation datasets. This is crucial in order to conduct further analysis and make reliable projections of future precipitation trends. (Figure S1). Although the CMIP6 historical runs cover the period of 1850–2014, we concentrated on historical simulations from 1951 to 2014.

Table 1. List of CMIP6 models, resolution, variant, and country information.

S. No.	CMIP6 Model Name	Horizontal Resolution (Long × Lat in Degrees)	Variant Label	Country of the Modeling Group
1	CESM2-WACCM	1.25 × 0.9375	r1i1p1f1	National Center for Atmospheric Research, USA
2	EC-Earth3	0.703125 × 0.703125	r1i1p1f1	EC-Earth-Consortium, Europe
3	EC-Earth3-Veg	0.703125 × 0.703125	r1i1p1f1	EC-Earth-Consortium, Europe
4	KACE-1-0-G	1.875 × 1.25	r1i1p1f1	National Institute of Meteorological Sciences (NIMS), National Institute of Meteorological Sciences (NIMS), Korea
5	KIOST-ESM	1.875 × 1.875	r1i1p1f1	Korea Institute of Ocean Science and Technology, Korea

Table 1. Cont.

S. No.	CMIP6 Model Name	Horizontal Resolution (Long × Lat in Degrees)	Variant Label	Country of the Modeling Group
6	MIROC6	1.40625 × 11.4516	r1i1p1f1	Japan Agency for Marine-Earth Science and Technology, Japan
7	MPI-ESM1-2-HR	0.9375 × 0.9375	r1i1p1f1	Max Planck Institute for Meteorology, Germany
8	NorESM2-LM	2.5 × 1.875	r1i1p1f1	Norwegian Meteorological Institute, Norway

2.4. Methodology

2.4.1. Downscaling and Empirical Quantile Mapping (EQM) Bias Correction

The morphology of the CMIP6 model used in our study has been tabulated in Table 1 of different resolutions. To facilitate bias correction, intercomparison, and model selection, all models were interpolated (using bilinear grid interpolation) to an IMD observation data grid ($0.25^\circ \times 0.25^\circ$). Statistical techniques are a vital tool in research applications for reducing systematic bias in the climate model simulations. It indicates that Empirical Quantile Mapping (EQM) is an effective approach for bias correction in climate model simulations [31]. It maps simulated and observed data in cumulative distribution functions (CDFs) that are empirically constructed based on historical data [40–42]. The adjustment on simulated data is performed by applying a linear mapping function between the observed and simulated quantiles. Therefore, prior to further analysis, EQM bias correction is applied to the historic simulation (1951–2014) and all three projected climate model scenarios SSP1-2.6 (2015–2100), SSP2-4.5 (2015–2100), and SSP5-8.5 (2015–2100). Python library Xclim (<https://xclim.readthedocs.io/en/stable/sdba.html> (accessed on 15 September 2022)) is used for the EQM bias correction [43]. The EQM bias correction factor was estimated for each grid and month and applied subsequently. EQM bias correction has been chosen as it is efficient and simple (Figures 2 and S2). Figure 2c,d indicate that the spatial correlation between the historical MME mean and IMD observed gridded product is greater than 0.3 in most regions, except for a few subdivisions such as Jammu and Kashmir, Madhya Maharashtra, N.I. Karnataka, and S.I. Karnataka. Furthermore, the root mean square error (RMSE) is less than 5 mm/day in most areas. The statistics suggest that the ensemble product shows strong agreement and less error with the observed data, which implies that there may be fewer uncertainties in future projections. The EQM method performance was found satisfactory and its detailed description and usage on different meteorological variables can be obtained in the recent literature (e.g., [31,42–44]).

2.4.2. Standard Precipitation Index (SPI)—Drought Index

The Standard Precipitation Index (SPI) is an important drought indicator for analyzing the likelihood of rainfall occurrence in a given region over a given time period [45]. It is highly sensitive to drought change and is useful in all drought assessments at various time scales. The SPI calculation for any location is based on a long-term precipitation record for a specified period of time. This long-term precipitation record is fitted to a probability distribution function (gamma or a Pearson Type III distribution), which is then converted into a normal distribution with the goal of achieving a mean SPI of zero for the location and desired period [46].

$$P_n^l = \sum_{i=0}^{l-1} (P_{n-i}), \quad n \geq 1 \quad (1)$$

where l is the aggregation timescale in months and n is the calculation number which must be $l \leq n$.

The Probability Distribution Function (PDF) of the gamma distribution for monthly precipitation (P) can be computed as follows:

$$f(P) = \frac{1}{\beta^\alpha \Gamma(\alpha)} P^{\alpha-1} e^{-\frac{P}{\beta}}, \quad \alpha, \beta > 0 \quad (2)$$

where $\Gamma(\alpha)$ is a gamma function and α and β are the shape and scale parameters, respectively. The probability distribution function (PDF) is calculated for each grid separately by considering independent datasets.

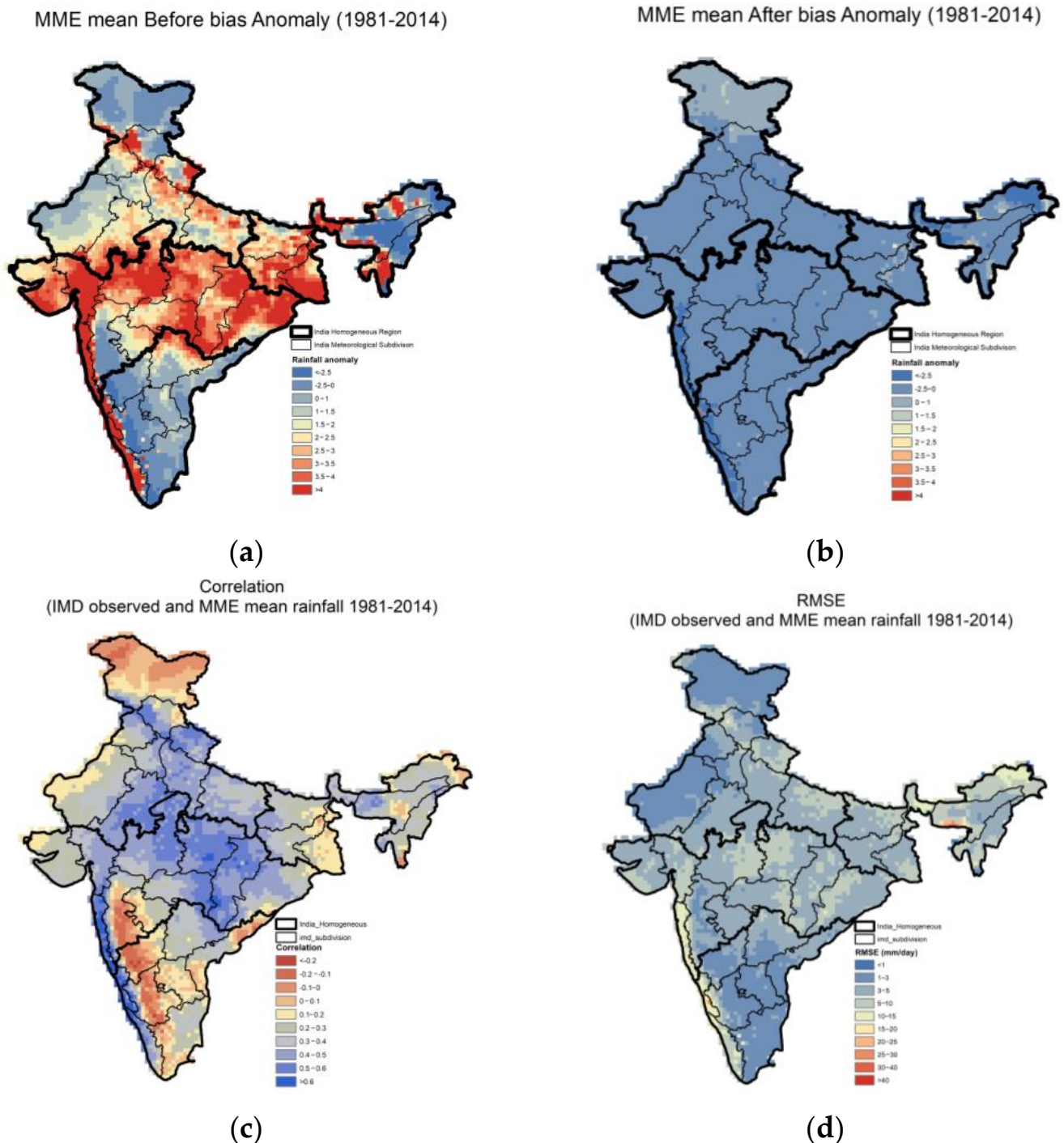


Figure 2. CMIP6 MME ensemble mean before and after EQM bias correction mean rainfall anomaly map; (a) before bias correction rainfall anomaly, (b) after bias correction rainfall anomaly, (c) correlation between IMD observed and bias-corrected CMIP6 ensemble mean rainfall (1981–2014), (d) RMSE between IMD observed and bias-corrected CMIP6 ensemble mean rainfall (1981–2014).

The SPI is dimensionless. Positive SPI values indicate that there is more precipitation than the median, while negative values indicate that there is less precipitation than the median. The SPI is normalized; therefore, we can assess both drier and wetter climates with the same index. The SPI is classified in the seven classes (Table 2) from extremely wet to extremely drought categories. The SPI is defined over the different timescales (1 month, 3 months, 6 months, up to 48 months) to address the different drought categories (meteorological drought, agricultural drought, hydrological drought, and socioeconomic drought).

Table 2. Standard Precipitation Index (SPI) categories.

SPI Range	SPI Category
<−2.0	Extreme Drought
−1.99 to −1.5	Severe Drought
−1.49 to −1.0	Moderate Drought
−0.99 to 0.99	Normal
1 to 1.49	Moderate Wet
1.5 to 1.99	Very Wet
>2.0	Extremely Wet

In the recent investigation, a 12-month SPI is estimated to address the agriculture drought and hydrological drought. The climate indices python library (<https://climate-indices.readthedocs.io/en/latest/> (accessed on 20 October 2022)) is used for the estimation of monthly SPI (gamma distribution) [45,47] for the historical period (1981–2014) as well as future SSPs scenarios (2015–2100). Following that, we applied mean zonal statistics to extract the meteorological subdivision level SPI data from gridded SPI data.

2.4.3. CMIP6 Bias Corrected Model Selection and Ensemble Product

Rajesh et al. (2022) [48] recommended eight best bias-corrected CMIP6 models based on a high correlation, similar spatial pattern, and close seasonal mean between the bias corrected models and IMD gridded observed datasets. The ensemble mean precipitation product has been prepared using the selected models. The drought index (SPI) has been estimated using the ensemble rainfall product of the SSPs scenarios.

The methodology used in this study is summarized in the flowchart (Figure 3). The CMIP6 data collected required pre-processing since each model's data were on a different grid (Table 1). To ensure consistency, all models were interpolated to the same spatial scale as the IMD gridded observed data. The EQM bias correction method was utilized to remove any biases in the CMIP6 model data, and the same correction factor was then applied to the SSP future scenarios of the CMIP6 data. To analyze decadal changes in the drought index over time, the IMD observed data were used to compute the drought index (SPI) for various time periods (1951–1980, 1961–1990, 1971–2000, 1981–2010, and 1991–2020). Additionally, the SPI was computed for the ensemble product of selected models of the CMIP6 historical data and all SSP future scenarios periods, including the near future (2023–2048), mid future (2049–2074), and far future (2075–2100).

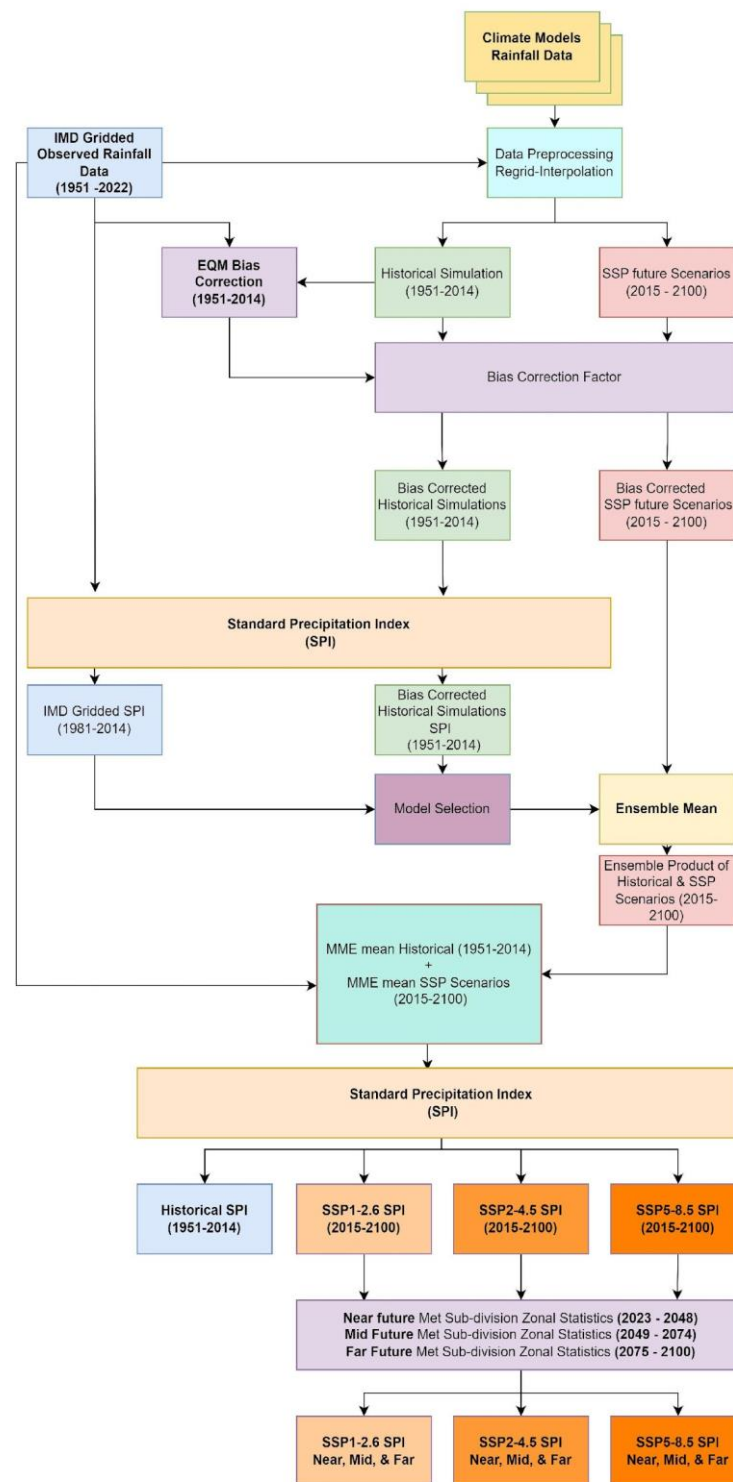


Figure 3. Flow chart of the designed investigation.

3. Results

3.1. Spatial–Temporal Variability of Observed Rainfall Climatology over Indian Sub-Continent

The spatial distribution of the mean (June to September) rainfall of the past 72 years (1951–2022) is shown in Figure 4. Evidently, as documented by several previous studies [36,49], the regional pattern of the monsoon season rainfall climatology is quite congruent with the rainfall data. A large variability has been observed in the spatial distribution of the monsoon rainfall (June to September) throughout the country. The met subdivisions of core monsoon regions, i.e., East and West Madhya Pradesh, Chhattisgarh, Odisha, and

Vidarbha, Northeast India subdivisions, and Western Ghat subdivisions i.e., Konkan and Goa, Coastal Karnataka, and Kerala, experience substantial monsoon rains with a rainfall of 8 mm/day or more during June to September. The Western Ghat and northeastern regions experience considerable rainfall because of their hilly topography, which condenses moisture-laden wind flow and causes precipitation there. As we move towards the north-west direction from the monsoon core region, the rainfall amount is decreased. The low and vulnerable rainfall zones are West and East Rajasthan, Rayalaseema, N. I. Karnataka, S. I. Karnataka, Tamil Nadu, and Jammu and Kashmir with a rainfall less than 4–5 mm/day during the monsoon season [6,50,51].

IMD Observed Mean Rainfall (JJAS) 1951-2022

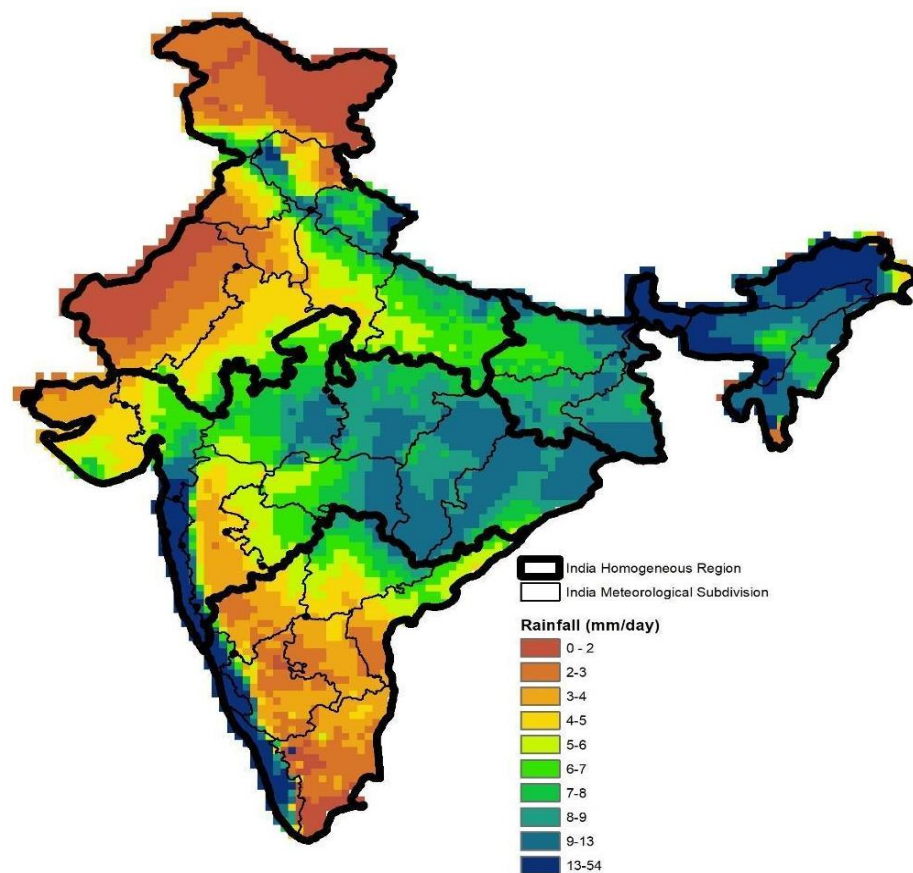


Figure 4. India Meteorological Department (IMD) Observed Rainfall (June to September) 1951–2022.

The IMD mean rainfall linear trend (JJAS) 1951–2022 (Figure 5) clearly shows that there is a significant decrease in monsoon rains over the monsoon core regions, specifically the met subdivisions East and West Uttar Pradesh, East Madhya Pradesh, Chhattisgarh, and Jharkhand. Saha et al.'s (2022) [44] study is also congruent with our findings on a decreasing trend of monsoon low pressure system frequency as well as a decrease in monsoon rainfall over the main monsoon core regions [52,53].

IMD Observed Mean Rainfall Trend (JJAS) 1951-2022

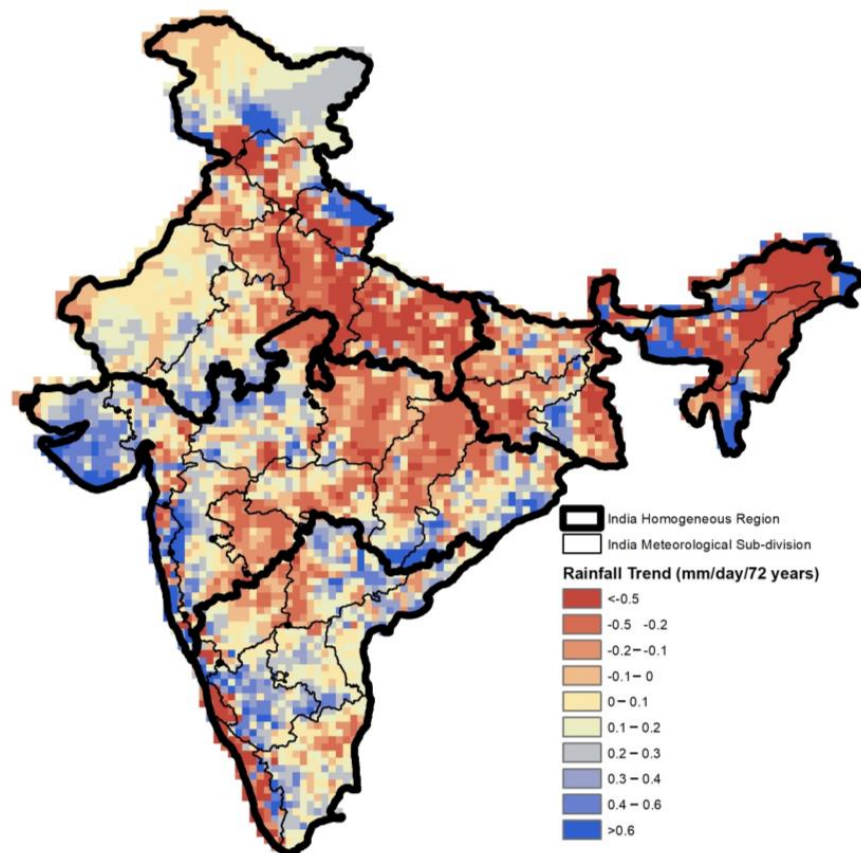


Figure 5. India Meteorological Department (IMD) Observed Mean Rainfall (June to September) Trend 1951–2022.

Other regions, i.e., most of the area of the northeastern states, Haryana, Marathwada, and the adjoining areas of North Interior Karnataka and Telangana, are experiencing a decrease in their rainfall trends in the last 72 years. Some regions are also experiencing an increase in rainfall trends such as Saurashtra and Kutch, the adjoining area of East Rajasthan and West Madhya Pradesh, the northern region of Uttarakhand, the western part of Assam and Meghalaya, the western region of Madhya Maharashtra, the adjoining area of South Chhattisgarh and Odisha, and South Interior Karnataka.

3.2. Inter Annual Variability of Monsoon Rainfall

The monsoon season is characterized by the onset, advancement, and withdrawal of monsoons during the season. Many sectors, i.e., agriculture, energy, environmental, etc., are affected or influenced by the interannual variability of extreme events. Therefore, a more detailed assessment of interannual variability and its causes is warranted, which also may help in planning to ameliorate the worst repercussions of extreme events. Interannual oscillations in the annual monsoon cycle cause unusually wet and dry years. Many studies have shown a strong relationship between the Indian monsoon and several indicators. These indicators include (1) internal dynamics such as atmospheric circulations that exhibit interannual variability, combined effects of dynamic instabilities (synoptic scale disturbances), a nonlinear interaction among various scales of motion, thermal, and orographic forcing tropical and extratropical interactions, and (2) the influence of global surface boundary conditions such as soil moisture, sea ice, snow cover, and sea surface temperature (SST), which can be assessed using various indices [6,44], i.e., El Nino Southern Oscillation (ENSO), the Indian Ocean Dipole (IOD), the North Atlantic Oscillation (NAO), and the

Pacific Decadal Oscillation (PDO). These indicators are the primary factors influencing the interannual variation of the southwest monsoon [54–56]. Figure 6a,b shows the interannual variability of southwest monsoons in rainfall departure percentage (%) and drought index SPI. Of the last 72 years (1951–2022), 30 years show a deficient rainfall departure (Figure 6a). A drought index SPI value below or equal to -1 indicates the deficient year. SPI boxplots (Figure 6b) depict a sinusoidal pattern of mean SPI across time, indicating that there is a pattern in interannual variability, with certain areas hit adversely in dry years. The extreme drought years of 1972, 1987, and 2002 are well captured in both rainfall departure and SPI analyses. In addition, the influence of these severe drought years has been observed in the immediate next year such as 1972 and 1973, 1987 and 1988, and 2002 and 2003 over the region as a variance of sample which is high.

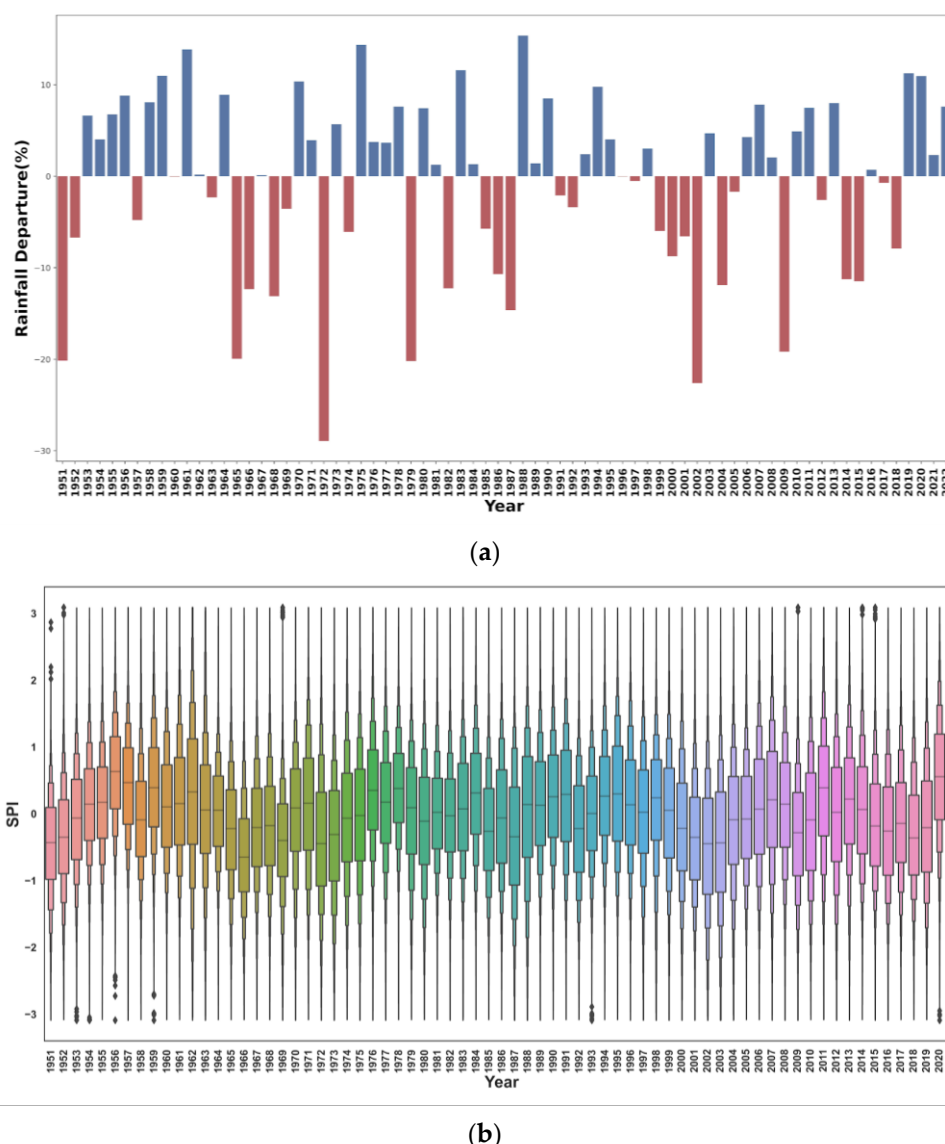


Figure 6. Interannual change in (a) rainfall departure in percentage (dry year in red color and wet year in blue color), (b) drought index (12-month Standard Precipitation Index) over Indian region for the period 1951–2021.

3.3. Decadal Variability of Dry and Wet Events

Decadal analysis is quite important to understand the changes in the dry/wet events frequency as well the shifting of the rainfall pattern for effective mitigation planning. The drought index at every meteorological subdivision level has been analyzed (Figure 7) and

the major changes in the recent two decades in a few subdivisions clearly observed. Central India is an ISM core region in which the Chhattisgarh and East MP met subdivisions' drought index have shifted significantly to the dry side in the past decade, and the results are in good agreement with the decreasing trend of ISM rainfall. There has been significant change in SPI observed over both the east and west coast of central India and over Conkan and Goa and Odisha in which the frequency of normal events are decreasing on a decadal basis and the SPI probability density curve (PDF) is skewed towards the wet side (right side) with a long tail (high extreme wet frequency) in recent decades. The West MP, Gujarat, Sourashtra, Marathwada, Vidarbha, and Madhya Maharashtra met subdivisions are susceptible to both wet and dry extreme events in the recent past decades.

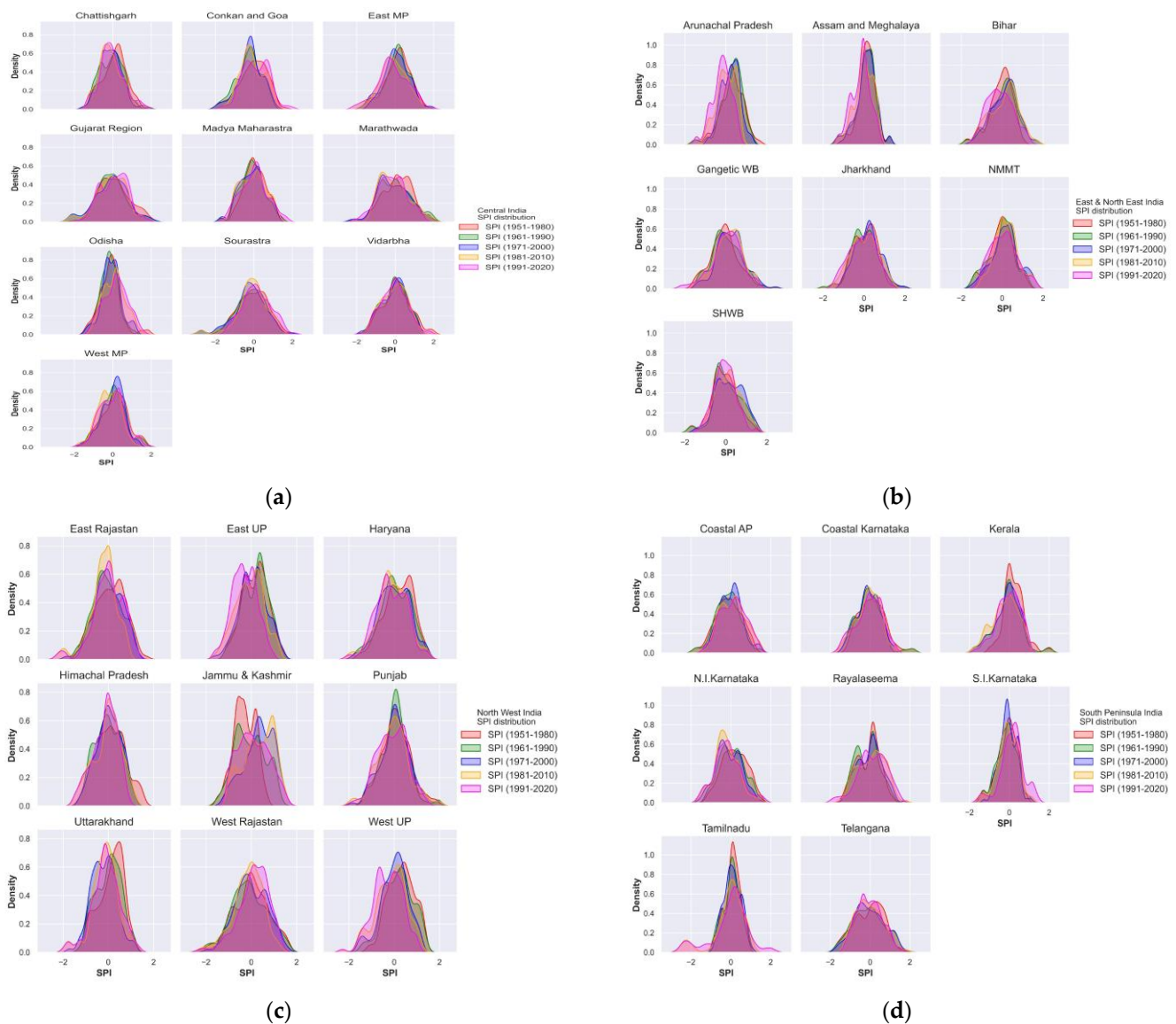


Figure 7. Interannual drought index decadal change probability density function (PDF) plot (a) Central India, (b) East and Northeast India, (c) Northwest India, and (d) South Peninsula India over Indian meteorological subdivision region for the period 1951–2020.

The northeast region consists mainly of hilly Himalayan region as well as Gangetic plains. The whole NE area drought index is shifting towards the dry side (Figure 7b), making it prone to drought occurrences, similar to the decreasing rainfall trend (Figure 5). The recent 30 years (1991–2020) SPI plot shows a large shift towards the dry side as well as a large decrease in probability of a normal drought index.

Northwest India has very high land variability consisting of arid, hilly, and Gangetic plains regions in which arid regions are highly susceptible to drought extreme events, and the recent decade drought index PDF plot clearly shows that East and West Rajasthan is right (wet side) skewed with a long tail towards the left (dry side), indicating a high likelihood of a normal year along with a high probability of severe drought risk. The Punjab and Haryana met subdivisions' PDF plot shows that normal event frequency is decreased with a longer tail on both sides, indicating that the frequency of droughts and floods has increased in recent decades. The drought index over hilly regions, the Jammu and Kashmir subdivisions, is erratic and unpredictable, but reflects a decreasing trend of normal events. The decreasing ISM rainfall trend throughout the Gangetic areas (East and West Uttar Pradesh) has been noticed in Figure 5; however, the similar sensitivity to the dry side has been exhibited in the drought index PDF plot (Figure 7), where the normal event frequency is shifting towards the dry side in recent decades.

The southwest monsoon is also significant over the South Peninsula region. However, the majority of the annual rainfall in certain southernmost regions of South Peninsula India occurs during the northeast monsoon (October to December). This region comprises both coastal and inland geographical areas. A significant change in the drought index has been noticed in the inland geographical areas in recent decades. The frequency of the normal drought index is reduced and an increase in the frequency of both dry and wet events is observed over N.I. Karnataka, S.I. Karnataka, Rayalaseema, and Telangana (Figure 7d). In the last decade, the Tamil Nadu met subdivision experienced extreme severe drought [57] and severe wet events, which are clearly portrayed in the drought index PDF plot. Over the Coastal AP and Coastal Karnataka subdivisions, a slight shift in normal event frequency towards the wet side has been observed, but over the Kerala subdivisions, there is a major shift in normal event frequency with a high frequency in dry events. Thus, in a nutshell, a substantial change in normal event frequency has been seen in most subdivisions over the last two decades, which is crucial for future risk and its mitigation assessments.

3.4. Bias-Corrected CMIP6 Projected Changes in the Frequency of Extreme Events (Dry/Wet)

As stated previously in the decadal analysis section, the uncertainty of dry and wet occurrences is increasing year-by-year, and future scenarios of the CMIP6 models indicate the same. CMIP6 ensemble rainfall anomalies for the future under SSP245 and SSP585 scenarios indicate that the concentration of rainfall is likely to increase in major pockets of central Madhya Pradesh, Bihar, the western coastal region of Concan and Goa, Coastal Karnataka, Chhattisgarh, Odisha, East Uttar Pradesh and East Rajasthan (Figure 8). The primary focus of the future projection study is an analysis of the probability of drought occurrence during the monsoon month (June to September). The CMIP6 model projections help to understand the risks of future extreme drought/wet events, its potential ramifications on various sectors, and risk mitigation policies designed at the regional level to minimize its negative impact. Future extreme events probability is analyzed using the kernel density estimation (KDE) and separate wet/dry event frequency analysis under different SSPs scenarios projections (SSP1-2.6, SSP2-4.5, and SSP5-8.5) for the periods of the near (2023–2048), mid (2049–2074), and far future (2075–2100). India is divided into four homogeneous regions based on coherent rainfall: East and Northeast, Northwest, Central, and South Peninsula India, which are further subdivided into 36 sub-meteorological zones. We conducted the study of climate change scenarios over the 34 major meteorological subdivisions (excluding Andaman and Nicobar Island and Lakshadweep).

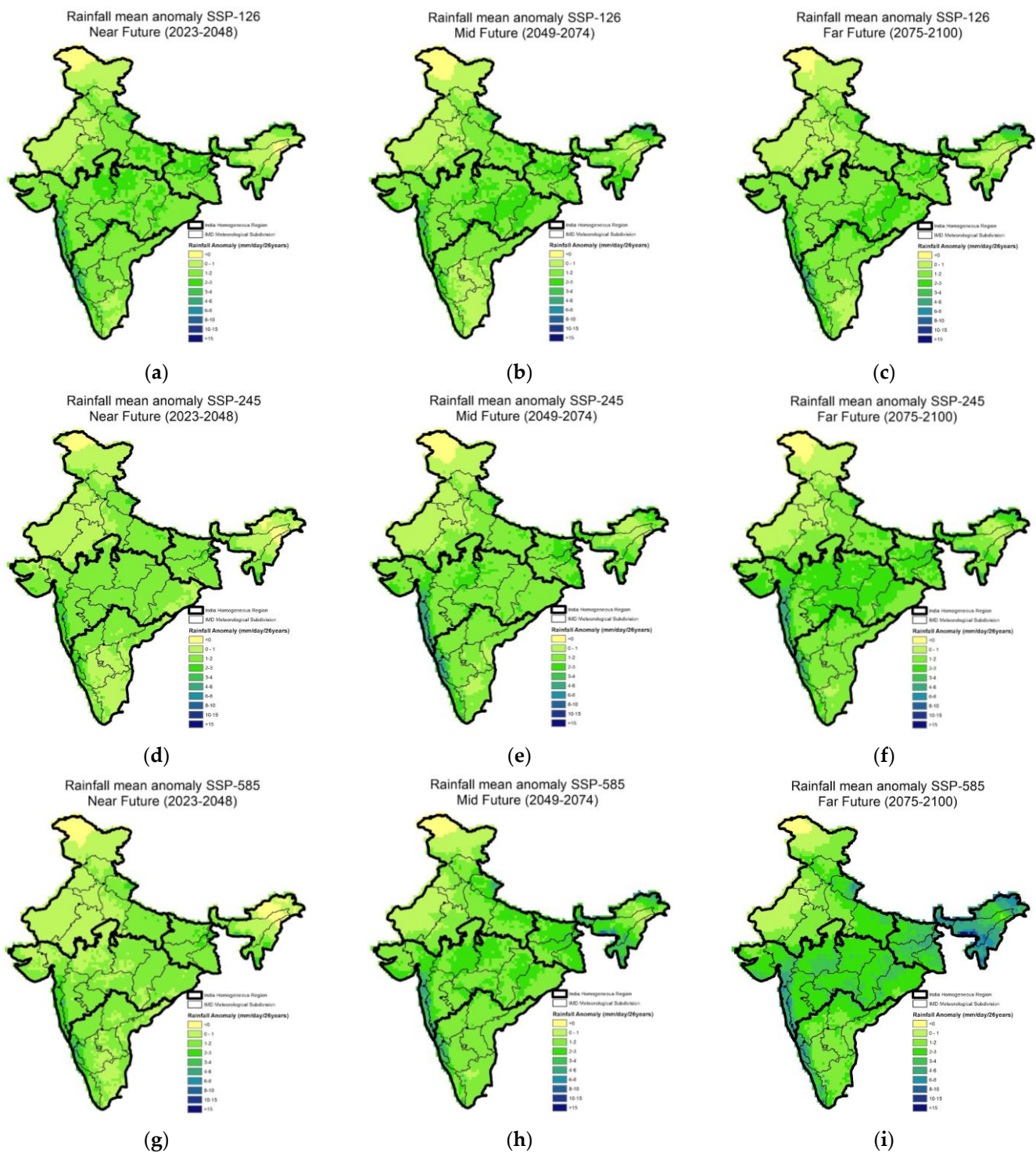


Figure 8. CMIP6 bias-corrected MME ensemble mean rainfall anomaly with reference to historical period (1989–2014) (a) mean rainfall anomaly SSP-126 Near future (2023–2048), (b) mean rainfall anomaly SSP-126 mid future (2049–2074), (c) mean rainfall anomaly SSP-126 far future (2075–2100), (d) mean rainfall anomaly SSP-245 near future (2023–2048), (e) mean rainfall anomaly SSP-245 mid future (2049–2074), (f) mean rainfall anomaly SSP-245 far future (2075–2100), (g) mean rainfall anomaly SSP-585 near future (2023–2048), (h) mean rainfall anomaly SSP-585 mid future (2049–2074), and (i) mean rainfall anomaly SSP-585 far future (2075–2100).

A main monsoon core region, the Central India homogeneous region’s SPI index median is most likely to shift towards the wet side with some extreme wet events and mod-

erate to severe dry events in the near future under SSP-126, SSP-245, and SSP585 scenarios (Figure 9a, Figure 10a, Figure 11a, and Figure 12a). If we drill down to the subdivision level, the frequency of occurrence of dry events (Figure 13) is likely to be moderate to severe drought frequency in the near future under the SSP-126 climatic scenario which is also likely to decrease in the mid and far future. Wet event frequency is comparatively high for West MP in the near future under the SSP126 scenarios (Figure 14). The wet frequency is likely to increase with extreme SSP scenarios in the mid and far future for all subdivisions of Central India. The East and Northeast India homogeneous regions are also in line with the Central India region and are likely to increase in wet event frequency in the mid and far future. The PDF plot (Figures 10–12) shows the more erratic SPI index distribution with the extreme SSP scenarios for the mid and far future.

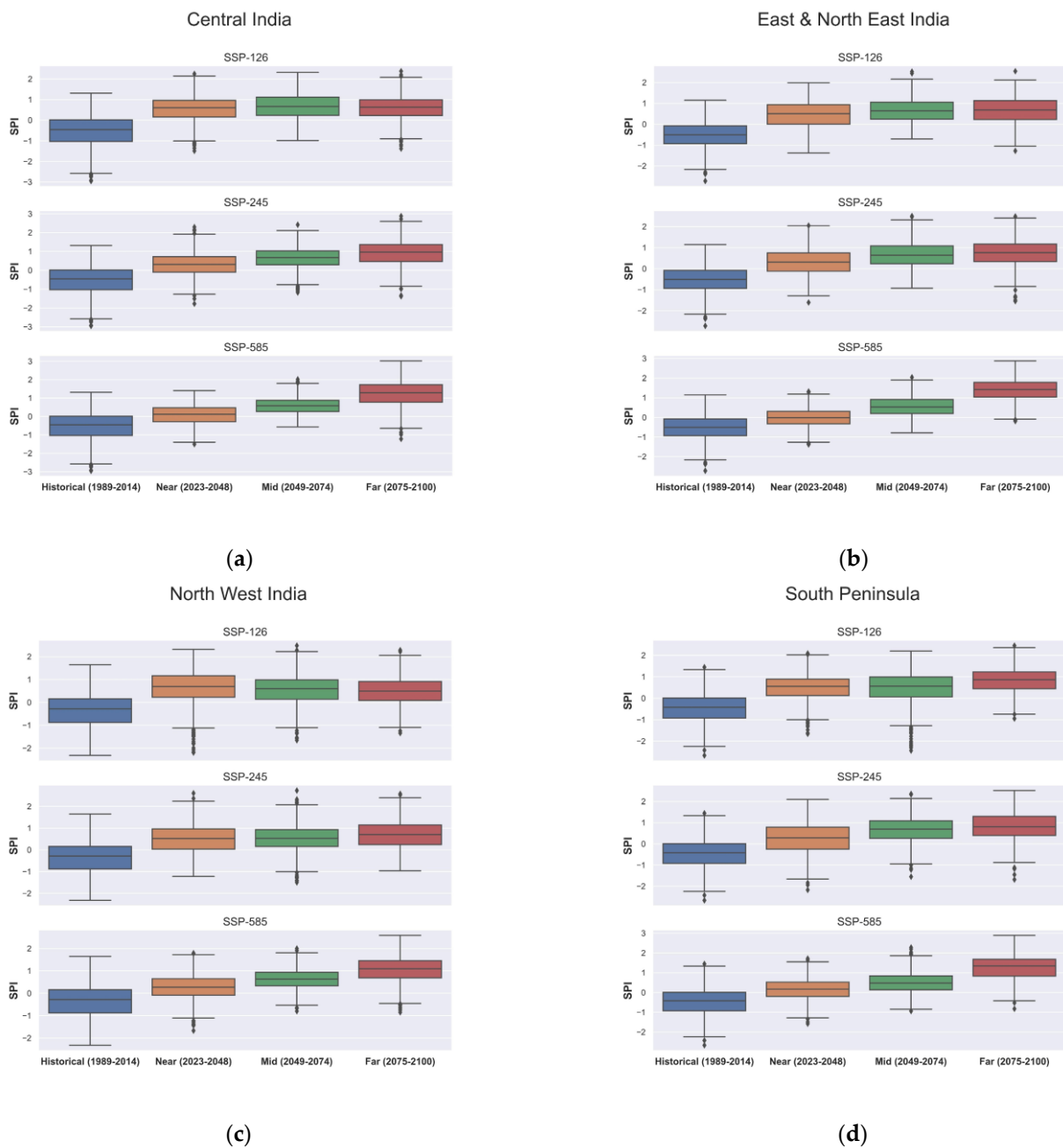


Figure 9. CMIP6 SSP scenarios 12-month Standard Precipitation Index (SPI) boxplot at homogeneous region level (a) Central India, (b) East and Northeast India, (c) Northwest India, and (d) South Peninsula India for near, mid, and far future.

Homogeneous regions such as Northwest India and South Peninsula India are likely to be impacted more than the Central and Northeast homogeneous region. Except Himachal Pradesh and Jammu and Kashmir, all subdivisions of Northwest India are vulnerable to severe drought events in the near future, especially Haryana, Punjab, West UP, and West and East Rajasthan (Figure 13). Figures 10c, 11c and 12c show the broader base of the probability density curve for both wet and dry, which indicate the erratic pattern of extreme events in the near future over the subdivisions of North West India. Figure 9c clearly illustrates that the frequency of wet events increases with the scenarios SSP-126, SSP-245, and SSP-585, and from the near to far future, similar to Central and North East India. South Peninsula subdivisions Coastal AP and Tamil Nadu are more susceptible to the drought events in the near future under all SSP scenarios and are likely to shift towards the wet extreme events in the mid and far future (Figure 14). Figures 10c, 11c and 12c show that the frequency of wet events is two-fold from the near future to mid future under the SSP-245 scenario.

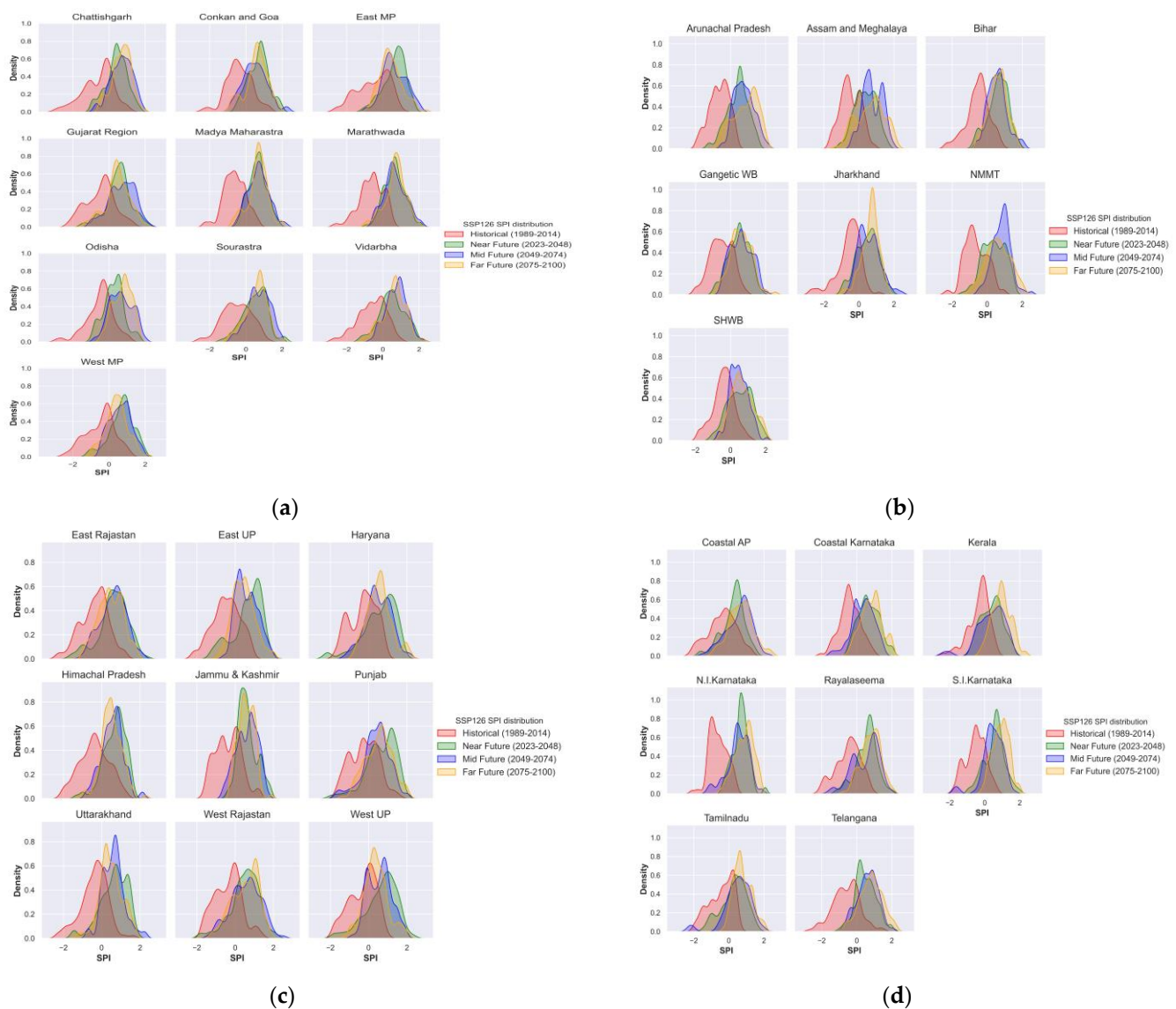


Figure 10. CMIP6 SSP126 scenarios 12-month Standard Precipitation Index (SPI) PDF plot at meteorological subdivision level (a) Central India, (b) East and Northeast India, (c) Northwest India, and (d) South Peninsula India for near, mid, and far future.

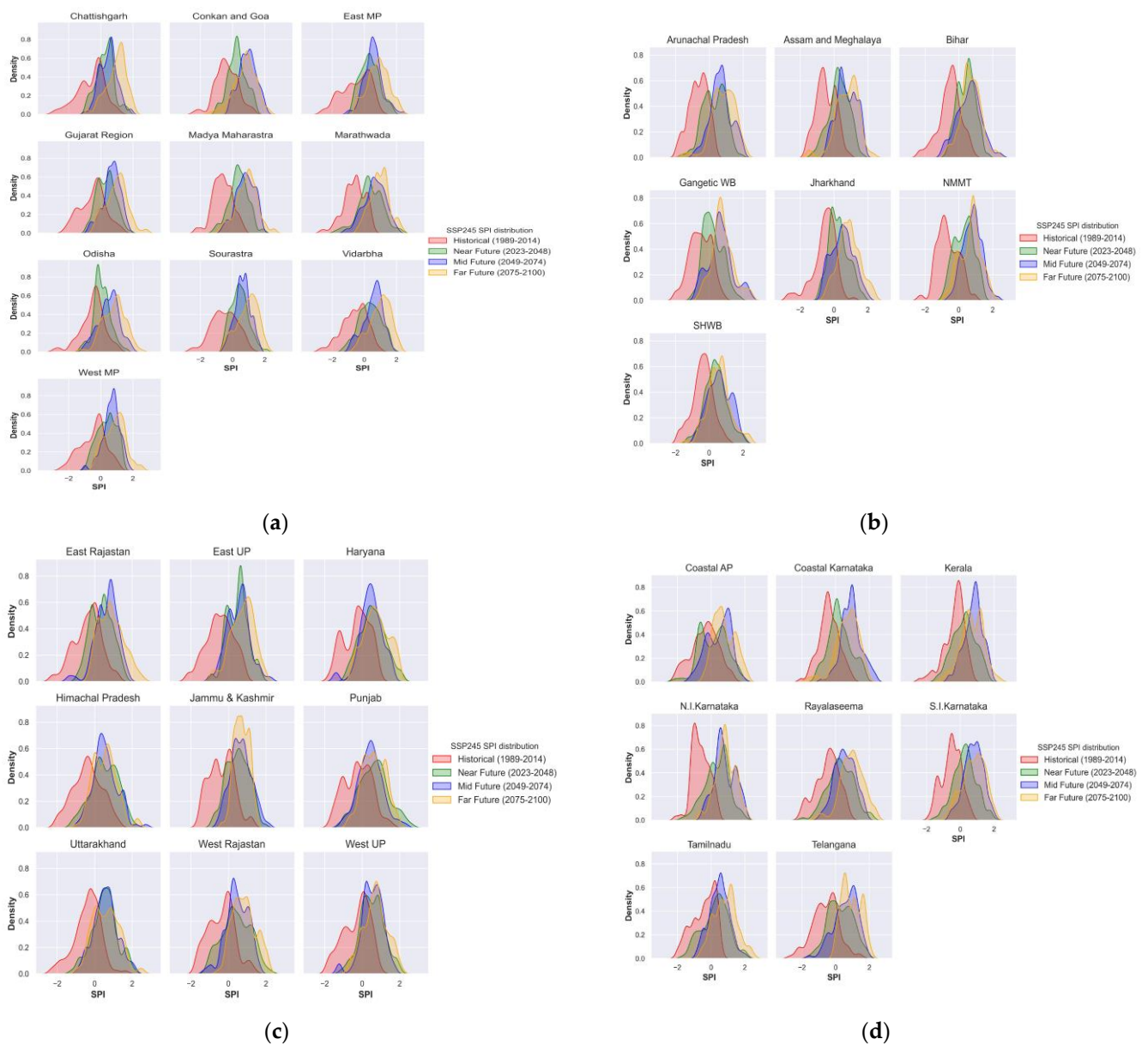


Figure 11. CMIP6 SSP245 scenarios 12-month Standard Precipitation Index (SPI) PDF plot at meteorological subdivision level (a) Central India, (b) East and Northeast India, (c) Northwest India, and (d) South Peninsula India for near, mid, and far future.

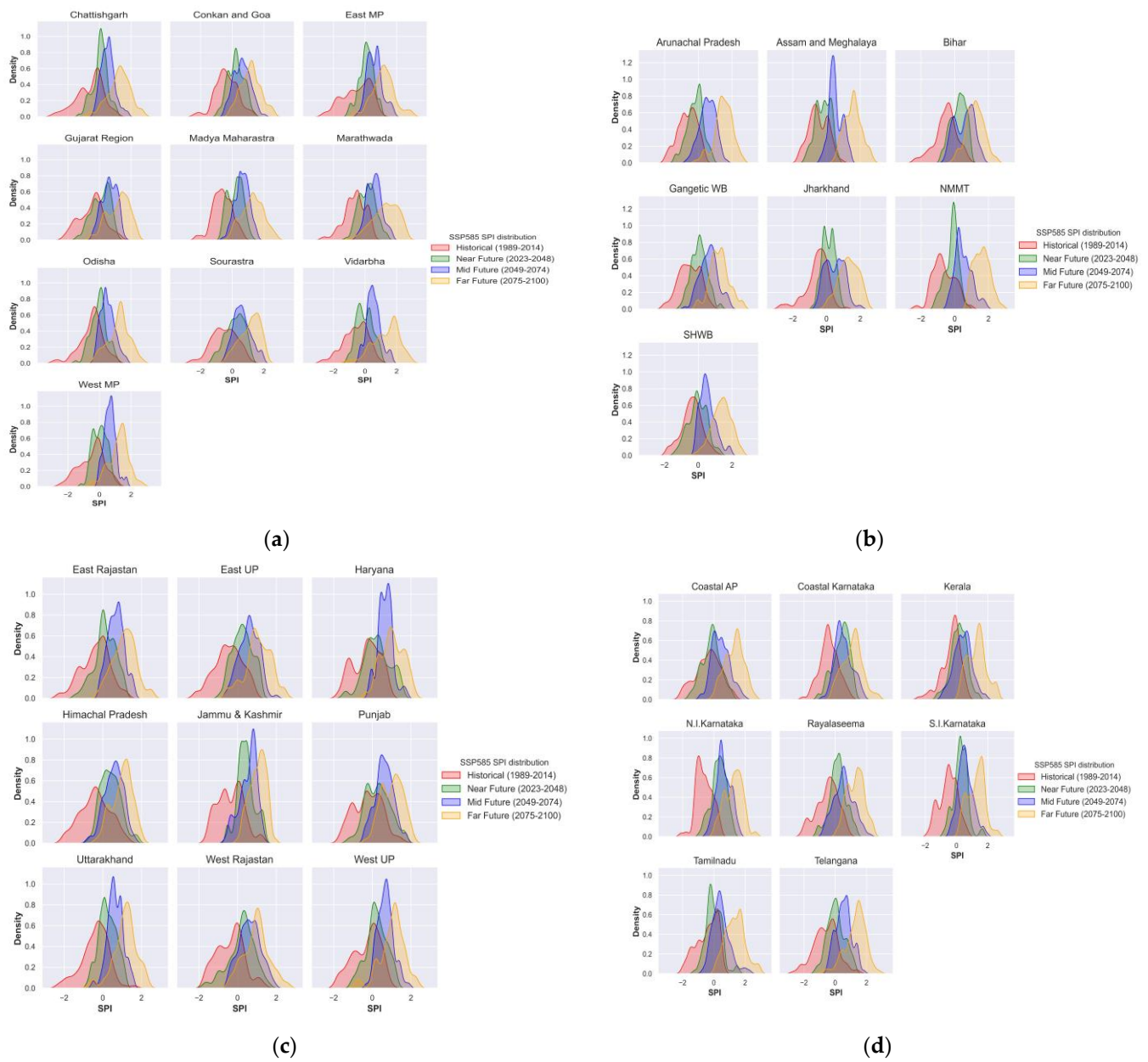


Figure 12. CMIP6 SSP585 scenarios 12-month Standard Precipitation Index (SPI) PDF plot at meteorological subdivision level (a) Central India, (b) East and Northeast India, (c) Northwest India, and (d) South Peninsula India for near, mid, and far future.

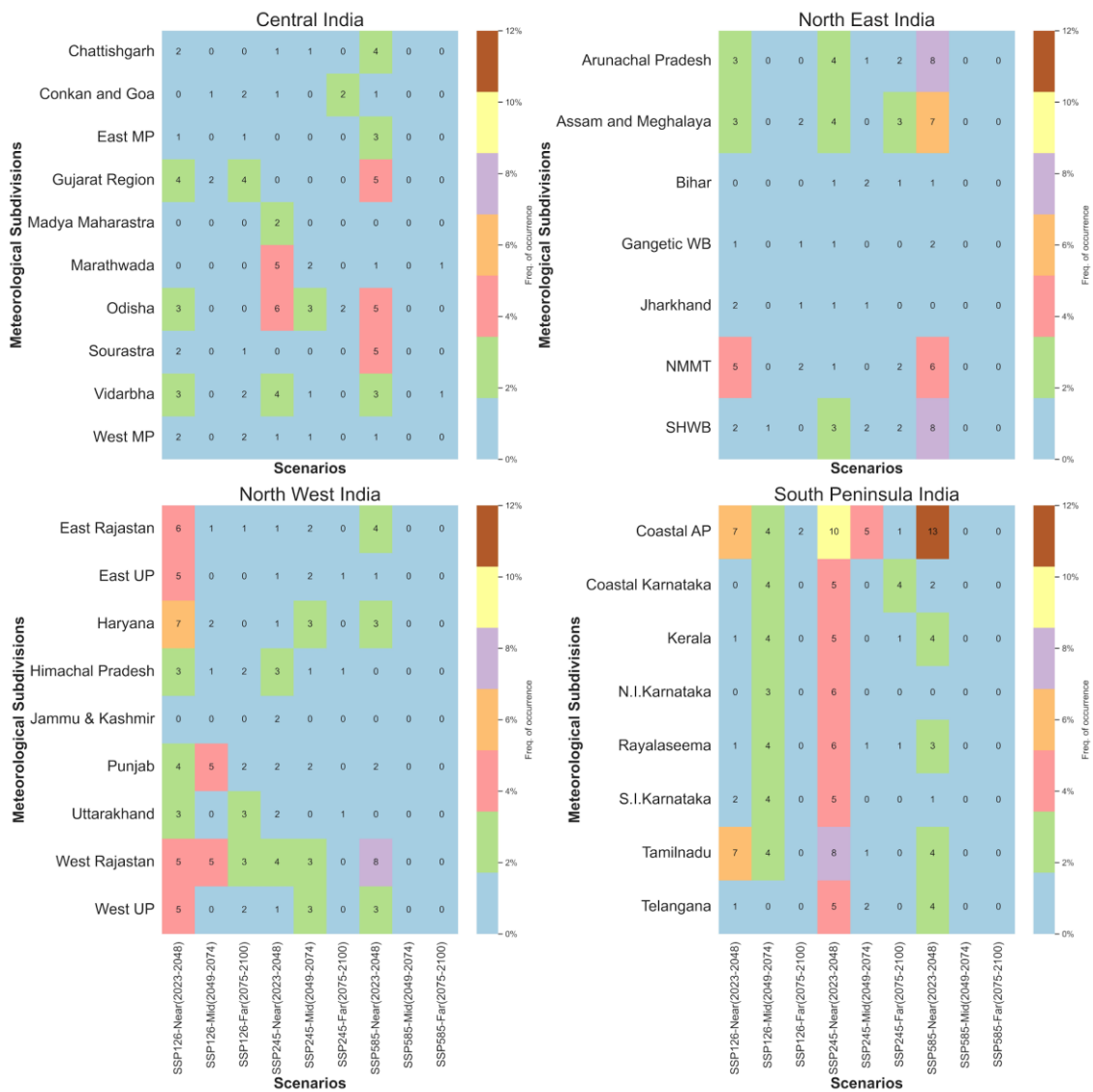


Figure 13. Frequency of occurrence (%) of drought events (12-month $SPI \leq -1.0$) at met subdivision level during the southwest monsoon months (June to September).

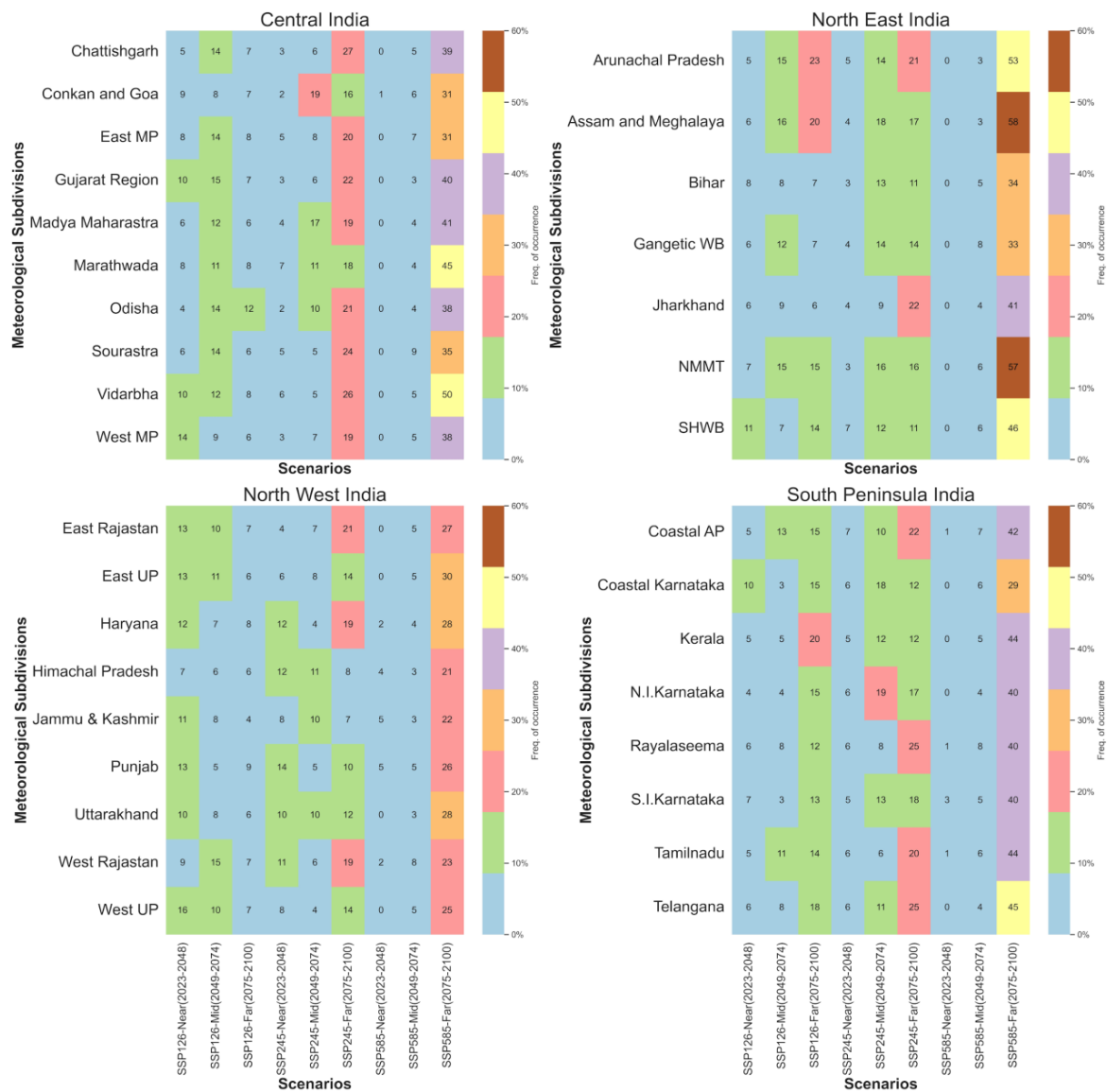


Figure 14. Frequency of occurrence (%) of wet events (12-month SPI \geq 1.5) at met subdivision level during the southwest monsoon months (June to September).

4. Summary and Conclusions

This paper discusses the spatial–temporal variability of observed rainfall climatology over the Indian subcontinent. The spatial distribution of the mean (June to September) rainfall for the past 72 years (1951–2022) is presented, indicating a large variability in the spatial distribution of monsoon rainfall throughout the country. Some regions are experiencing a decrease in the rainfall trend in the last 72 years, while other regions are experiencing an increase in the rainfall trend. This paper also discusses the interannual variability of monsoon rainfall and the relationship between the Indian monsoon and several indicators. This paper presents the interannual variability of the southwest monsoon in rainfall departure percentage and drought index SPI. Finally, the study analyzes the decadal variability of dry and wet events in the past, and also examines the projected variability of these events in the near, mid, and far future under various SSP pathways, with the aim of facilitating effective mitigation planning.

The findings aid in comprehending the past trends and variations in the frequency of extreme dry/wet events and their correlation with future projections for various SSP scenarios at the met subdivision level. This comprehension enables improved assessments of vulnerable subdivisions and the effective implementation of mechanisms to mitigate

future risks. The increase in drought frequency could lead to various possible consequences, such as water scarcity, agricultural losses, economic setbacks, health impacts, and environmental degradation. Analyzing the causes of drought is crucial in mitigating its worst impacts. These causes can be natural or anthropogenic factors (i.e., excessive water demand, deforestation, irrigation, etc.), or a combination of both [58]. Recent experiences of the consequences of drought can also help effective planning and decision-making such as implementing water conservation and management strategies, promoting sustainable agriculture practices, developing contingency plans for water shortages, etc. Our study suggests that subdivisions in Northwest India and South Peninsula India are particularly vulnerable in the future to droughts, given their existing drought-prone conditions. Therefore, it is imperative to develop appropriate mitigation strategies to address the risks associated with droughts in these regions.

The findings of this study can also significantly contribute to the global understanding of climate change and its impacts on extreme events. The study's regional understanding of the Indian subcontinent can complement the global understanding of climate change impacts by providing a more detailed and context-specific analysis of the impacts on a particular region. Additionally, the study uses a novel approach that combines the analysis of observational data and climate model projections at the meteorological subdivision level. This approach can help to improve the accuracy and reliability of global climate models.

Supplementary Materials: The following supporting information can be downloaded at: <https://www.mdpi.com/article/10.3390/atmos14040725/s1>, Figure S1: Without bias-corrected CMIP6 Model Rainfall Data for the Period 1981–2014; Figure S2: EQM Bias-corrected CMIP6 Model Rainfall Data for the Period 1981–2014.

Author Contributions: Conceptualization, A.K.S., M.S., J.N.T. and M.T.; methodology, A.K.S., M.S. and T.S.; software, A.K.S. and M.S.; validation, M.S., A.K.S. and T.S.; formal analysis, J.N.T.; investigation, M.T. and J.N.T.; writing—original draft preparation, A.K.S.; writing—review and editing, A.K.S., M.T. and T.S.; visualization, M.S.; supervision, J.N.T. and M.T. All authors have read and agreed to the published version of the manuscript.

Funding: This research received no external funding.

Institutional Review Board Statement: Not applicable.

Informed Consent Statement: Not applicable.

Data Availability Statement: The data that support the findings of this study are available from the corresponding author upon reasonable request.

Acknowledgments: The authors thank the India Meteorological Department (IMD) and World Climate Research Program (WCRP) for making the IMD gridded rainfall dataset and CMIP6 dataset, respectively, and made readily available for research. The authors also thankfully acknowledge Upal Saha, Project Scientist III at NCMRWE, Noida for his constant support, guidance, and encouragement for carrying out this work.

Conflicts of Interest: The authors declare no conflict of interest and no funders had any role in the design of the study; in the collection, analyses, or interpretation of data; in the writing of the manuscript; or in the decision to publish the results.

References

1. Census of India. 2011. Available online: <https://censusindia.gov.in/nada/index.php/catalog/1130> (accessed on 1 November 2022).
2. Bachmair, S.; Kohn, I.; Stahl, K. Exploring the link between drought indicators and impacts. *Nat. Hazards Earth Syst. Sci.* **2015**, *15*, 1381–1397. [[CrossRef](#)]
3. Mukherjee, S.; Aadhar, S.; Stone, D.; Mishra, V. Increase in extreme precipitation events under anthropogenic warming in India. *Weather Clim. Extrem.* **2018**, *20*, 45–53. [[CrossRef](#)]
4. Sankriti, R.; Saravanan, S.; Aluru, M.; Singh, L.; Jennifer, J.J.; Abijith, D. Chapter 16—Identification of drought intensity and development of drought resilience in the Rayalaseema region of Andhra Pradesh, India. In *Disaster Resilience and Sustainability*; Pal, I., Shaw, R., Djalante, R., Shrestha, S., Eds.; Elsevier: Amsterdam, The Netherlands, 2021; pp. 357–377. [[CrossRef](#)]

5. Vogt, J.V.; Safriel, U.; von Maltitz, G.; Sokona, Y.; Zougmore, R.; Bastin, G.; Hill, J. Monitoring and assessment of land degradation and desertification: Towards new conceptual and integrated approaches. *Land Degrad. Dev.* **2011**, *22*, 150–165. [[CrossRef](#)]
6. Rajeevan, M.N.; Nayak, S. *Springer Geology Observed Climate Variability and Change over the Indian Region*; Springer EBooks; Springer: Singapore, 2017; Available online: <http://www.myilibrary.com?id=968509> (accessed on 19 March 2023).
7. Ghorbanpour, A.K.; Afshar, A.; Hessels, T.; Duan, Z. Water and productivity accounting using WA+ framework for sustainable water resources management: Case study of northwestern Iran. *Phys. Chem. Earth* **2022**, *128*, 103245. [[CrossRef](#)]
8. Khatiwada, K.R.; Pandey, V.P. Characterization of hydro-meteorological drought in Nepal Himalaya: A case of Karnali River Basin. *Weather Clim. Extrem.* **2019**, *26*, 100239. [[CrossRef](#)]
9. Trambauer, P.; Maskey, S.; Werner, M.; Pappenberger, F.; van Beek, L.P.H.; Uhlenbrook, S. Identification and simulation of space–time variability of past hydrological drought events in the Limpopo River basin, southern Africa. *Hydrol. Earth Syst. Sci.* **2014**, *18*, 2925–2942. [[CrossRef](#)]
10. Uhe, P.; Philip, S.; Kew, S.; Shah, K.; Kimutai, J.; Mwangi, E.; van Oldenborgh, G.J.; Singh, R.; Arrighi, J.; Jjemba, E.; et al. Attributing drivers of the 2016 Kenyan drought. *Int. J. Climatol.* **2018**, *38*, e554–e568. [[CrossRef](#)]
11. Wambura, F.J. Uncertainty of drought information in a data-scarce tropical river basin. *J. Hydrol. Reg. Stud.* **2020**, *32*, 100760. [[CrossRef](#)]
12. Chan, S.S.; Seidenfaden, I.K.; Jensen, K.H.; Sonnenborg, T.O. Climate change impacts and uncertainty on spatiotemporal variations of drought indices for an irrigated catchment. *J. Hydrol.* **2021**, *601*, 126814. [[CrossRef](#)]
13. Saharwardi, M.S.; Kumar, P. Future drought changes and associated uncertainty over the homogenous regions of India: A multi-model approach. *Int. J. Climatol.* **2022**, *42*, 652–670. [[CrossRef](#)]
14. Kulkarni, A. Weakening of Indian summer monsoon rainfall in warming environment. *Theor. Appl. Climatol.* **2012**, *109*, 447–459. [[CrossRef](#)]
15. Pattanaik, D.R.; Rajeevan, M. Variability of extreme rainfall events over India during southwest monsoon season. *Meteorol. Appl.* **2010**, *17*, 88–104. [[CrossRef](#)]
16. Saha, A.; Ghosh, S. Can the weakening of Indian Monsoon be attributed to anthropogenic aerosols? *Environ. Res. Commun.* **2019**, *1*, 61006. [[CrossRef](#)]
17. Kchouk, S.; Melsen, L.A.; Walker, D.W.; van Oel, P.R. A review of drought indices: Predominance of drivers over impacts and the importance of local context. *Nat. Hazards Earth Syst. Sci. Discuss.* **2021**, 1–28. [[CrossRef](#)]
18. Niranjana Kumar, K.; Rajeevan, M.; Pai, D.S.; Srivastava, A.K.; Preethi, B. On the observed variability of monsoon droughts over India. *Weather Clim. Extrem.* **2013**, *1*, 42–50. [[CrossRef](#)]
19. O'Neill, B.C.; Tebaldi, C.; van Vuuren, D.P.; Eyring, V.; Friedlingstein, P.; Hurtt, G.; Knutti, R.; Kriegler, E.; Lamarque, J.F.; Lowe, J.; et al. The Scenario Model Intercomparison Project (ScenarioMIP) for CMIP6. *Geosci. Model Dev.* **2016**, *9*, 3461–3482. [[CrossRef](#)]
20. Riahi, K.; van Vuuren, D.P.; Kriegler, E.; Edmonds, J.; O'Neill, B.C.; Fujimori, S.; Bauer, N.; Calvin, K.; Dellink, R.; Fricko, O.; et al. The Shared Socioeconomic Pathways and their energy, land use, and greenhouse gas emissions implications: An overview. *Glob. Environ. Chang.* **2017**, *42*, 153–168. [[CrossRef](#)]
21. Ayugi, B.; Zhihong, J.; Zhu, H.; Ngoma, H.; Babausmail, H.; Rizwan, K.; Dike, V. Comparison of CMIP6 and CMIP5 models in simulating mean and extreme precipitation over East Africa. *Int. J. Climatol.* **2021**, *41*, 6474–6496. [[CrossRef](#)]
22. Dutta, U.; Hazra, A.; Chaudhari, H.S.; Saha, S.K.; Pokhrel, S.; Verma, U. Unraveling the global teleconnections of Indian summer monsoon clouds: Expedition from CMIP5 to CMIP6. *Glob. Planet. Chang.* **2022**, *215*, 103873. [[CrossRef](#)]
23. Gusain, A.; Ghosh, S.; Karmakar, S. Added value of CMIP6 over CMIP5 models in simulating Indian summer monsoon rainfall. *Atmos. Res.* **2020**, *232*, 104680. [[CrossRef](#)]
24. Hamed, M.M.; Nashwan, M.S.; Shahid, S.; bin Ismail, T.; Wang, X.; Dewan, A.; Asaduzzaman, M. Inconsistency in historical simulations and future projections of temperature and rainfall: A comparison of CMIP5 and CMIP6 models over Southeast Asia. *Atmos. Res.* **2022**, *265*, 105927. [[CrossRef](#)]
25. Eyring, V.; Bony, S.; Meehl, G.A.; Senior, C.A.; Stevens, B.; Stouffer, R.J.; Taylor, K.E. Overview of the Coupled Model Intercomparison Project Phase 6 (CMIP6) experimental design and organization. *Geosci. Model Dev.* **2016**, *9*, 1937–1958. [[CrossRef](#)]
26. Rajbanshi, J.; Das, S. The variability and teleconnections of meteorological drought in the Indian summer monsoon season: Implications for staple crop production. *J. Hydrol.* **2021**, *603*, 126845. [[CrossRef](#)]
27. Aadhar, S.; Mishra, V. Challenges in drought monitoring and assessment in India. *Water Secur.* **2022**, *16*, 100120. [[CrossRef](#)]
28. Arunrat, N.; Sereenonchai, S.; Chaowiwat, W.; Wang, C. Climate change impact on major crop yield and water footprint under CMIP6 climate projections in repeated drought and flood areas in Thailand. *Sci. Total Environ.* **2022**, *807*, 150741. [[CrossRef](#)] [[PubMed](#)]
29. Katzenberger, A.; Schewe, J.; Pongratz, J.; Levermann, A. Robust increase of Indian monsoon rainfall and its variability under future warming in CMIP6 models. *Earth Syst. Dyn.* **2021**, *12*, 367–386. [[CrossRef](#)]
30. Li, X.; Tan, L.; Li, Y.; Qi, J.; Feng, P.; Li, B.; Liu, D.L.; Zhang, X.; Marek, G.W.; Zhang, Y.; et al. Effects of global climate change on the hydrological cycle and crop growth under heavily irrigated management—A comparison between CMIP5 and CMIP6. *Comput. Electron. Agric.* **2022**, *202*, 107408. [[CrossRef](#)]
31. Mishra, V.; Bhatia, U.; Tiwari, A.D. Bias-corrected climate projections for South Asia from Coupled Model Intercomparison Project-6. *Sci. Data* **2020**, *7*, 338. [[CrossRef](#)]
32. Mondal, S.K.; Huang, J.; Wang, Y.; Su, B.; Zhai, J.; Tao, H.; Wang, G.; Fischer, T.; Wen, S.; Jiang, T. Doubling of the population exposed to drought over South Asia: CMIP6 multi-model-based analysis. *Sci. Total Environ.* **2021**, *771*, 145186. [[CrossRef](#)]

33. Sreeparvathy, V.; Srinivas, V.V. Meteorological flash droughts risk projections based on CMIP6 climate change scenarios. *NPJ Clim. Atmos. Sci.* **2022**, *5*, 77. [[CrossRef](#)]
34. Wang, T.; Tu, X.; Singh, V.P.; Chen, X.; Lin, K. Global data assessment and analysis of drought characteristics based on CMIP6. *J. Hydrol.* **2021**, *596*, 126091. [[CrossRef](#)]
35. Zhai, J.; Mondal, S.K.; Fischer, T.; Wang, Y.; Su, B.; Huang, J.; Tao, H.; Wang, G.; Ullah, W.; Uddin, M.d.J. Future drought characteristics through a multi-model ensemble from CMIP6 over South Asia. *Atmos. Res.* **2020**, *246*, 105111. [[CrossRef](#)]
36. Pai, D.S.; Sridhar, L.; Rajeevan, M.; Sreejith, O.P.; Satbhai, N.S.; Mukhopadhyay, B. Development of a new high spatial resolution ($0.25^\circ \times 0.25^\circ$) long period (1901–2010) daily gridded rainfall data set over India and its comparison with existing data sets over the region. *Mausam* **2014**, *65*, 1–18. [[CrossRef](#)]
37. Jena, P.; Garg, S.; Azad, S. Performance analysis of imd high-resolution gridded rainfall ($0.25^\circ \times 0.25^\circ$) and satellite estimates for detecting cloudburst events over the Northwest Himalayas. *J. Hydrometeorol.* **2020**, *21*, 1549. [[CrossRef](#)]
38. Rajeevan, M.; Bhate, J.; Kale, J.D.; Lal, B. High resolution daily gridded rainfall data for the Indian region: Analysis of break and active monsoon spells. *Curr. Sci.* **2008**, *91*, 296–306.
39. Yatagai, A.; Kamiguchi, K.; Arakawa, O.; Hamada, A.; Yasutomi, N.; Kitoh, A. Aphrodite constructing a long-term daily gridded precipitation dataset for Asia based on a dense network of rain gauges. *Bull. Am. Meteorol. Soc.* **2012**, *93*, 1401–1415. [[CrossRef](#)]
40. Agbazo, M.N.; Grenier, P. Characterizing and avoiding physical inconsistency generated by the application of univariate quantile mapping on daily minimum and maximum temperatures over Hudson Bay. *Int. J. Climatol.* **2020**, *40*, 3868–3884. [[CrossRef](#)]
41. Hoffmann, H.; Rath, T. Meteorologically consistent bias correction of climate time series for agricultural models. *Theor. Appl. Climatol.* **2012**, *110*, 129–141. [[CrossRef](#)]
42. Thrasher, B.; Maurer, E.P.; McKellar, C.; Duffy, P.B. Technical Note: Bias correcting climate model simulated daily temperature extremes with quantile mapping. *Hydrol. Earth Syst. Sci.* **2012**, *16*, 3309–3314. [[CrossRef](#)]
43. Déqué, M. Frequency of precipitation and temperature extremes over France in an anthropogenic scenario: Model results and statistical correction according to observed values. *Glob. Planet. Chang.* **2007**, *57*, 16–26. [[CrossRef](#)]
44. Saha, U.; Sateesh, M. Rainfall extremes on the rise: Observations during 1951–2020 and bias-corrected CMIP6 projections for near- and late 21st century over Indian landmass. *J. Hydrol.* **2022**, *608*, 127682. [[CrossRef](#)]
45. Mckee, T.B.; Doesken, N.J.; Kleist, J. The relationship of drought frequency and duration to time scales. In Proceedings of the Eighth Conference on Applied Climatology, Anaheim, CA, USA, 17–22 January 1993.
46. Edwards, D.C.; Mckee, T.B. *Characteristics of 20th Century Drought in the United States at Multiple Time Scales*; Atmospheric Science Paper; Colorado State University: Fort Collins, CO, USA, 1997; Volume 634, pp. 1–30. Available online: <https://mountainscholar.org/handle/10217/170176> (accessed on 19 March 2023).
47. Hayes, M.; Svoboda, M.; Wall, N.; Widhalm, M. The lincoln declaration on drought indices: Universal meteorological drought index recommended. *Bull. Am. Meteorol. Soc.* **2011**, *92*, 485–488. [[CrossRef](#)]
48. Rajesh, P.; Goswami, B.N. Climate Change and Potential Demise of the Indian Deserts. *arXiv* **2022**, arXiv:2212.13711. [[CrossRef](#)]
49. Pal, L.; Ojha, C.S.P.; Dimri, A.P. Characterizing rainfall occurrence in India: Natural variability and recent trends. *J. Hydrol.* **2021**, *603*, 126979. [[CrossRef](#)]
50. Guhathakurta, P.; Rajeevan, M. Trends in the rainfall pattern over India. *Int. J. Climatol.* **2008**, *28*, 1453–1469. [[CrossRef](#)]
51. Guhathakurta, P.; Menon, P.; Inkane, P.M.; Krishnan, U.; Sable, S.T. Trends and variability of meteorological drought over the districts of India using standardized precipitation index. *J. Earth Syst. Sci.* **2017**, *126*, 120. [[CrossRef](#)]
52. Krishnamurthy, V.; Ajayamohan, R.S. Composite Structure of Monsoon Low Pressure Systems and Its Relation to Indian Rainfall. *J. Clim.* **2010**, *23*, 4285–4305. [[CrossRef](#)]
53. Vishnu, S.; Boos, W.R.; Ullrich, P.A.; O'Brien, T.A. Assessing Historical Variability of South Asian Monsoon Lows and Depressions With an Optimized Tracking Algorithm. *J. Geophys. Res. Atmos.* **2020**, *125*, e2020JD032977. [[CrossRef](#)]
54. Bal, P.K.; Dasari, H.P.; Prasad, N.; Salunke, P.; Parihar, R.S. Variations of Energy Fluxes with ENSO, IOD and ISV of Indian Summer Monsoon Rainfall over the Indian Monsoon Region. *Atmos. Res.* **2021**, *258*, 105645. [[CrossRef](#)]
55. Saha, K.; Guha, A.; Banik, T. Indian summer monsoon variability over North-East India: Impact of ENSO and IOD. *J. Atmos. Sol.-Terr. Phys.* **2021**, *221*, 105705. [[CrossRef](#)]
56. Sankar, S.; Vijaykumar, P.; Abhilash, S.; Mohanakumar, K. Influence of the strongest positive Indian Ocean Dipole and an El Niño Modoki event on the 2019 Indian summer monsoon. *Dyn. Atmos. Ocean.* **2021**, *95*, 101235. [[CrossRef](#)]
57. Mishra, V.; Thirumalai, K.; Jain, S.; Aadhar, S. Unprecedented drought in South India and recent water scarcity. *Environ. Res. Lett.* **2021**, *16*, 054007. [[CrossRef](#)]
58. Bonacci, O.; Bonacci, D.; Roje-Bonacci, T.; Vrsalovic, A. Proposal of a new method for drought analysis. *J. Hydrol. Hydromech.* **2023**, *71*, 100–110. [[CrossRef](#)]

Disclaimer/Publisher's Note: The statements, opinions and data contained in all publications are solely those of the individual author(s) and contributor(s) and not of MDPI and/or the editor(s). MDPI and/or the editor(s) disclaim responsibility for any injury to people or property resulting from any ideas, methods, instructions or products referred to in the content.